Reversible Thermal Unfolding of Ribonuclease T_1 in Reverse Micelles[†]

M. C. R. Shastry and M. R. Eftink*

Department of Chemistry, University of Mississippi, University, Mississippi 38677

Received October 26, 1995; Revised Manuscript Received January 29, 1996[⊗]

ABSTRACT: The reverse micellar system formed by the negatively charged surfactant AOT and the organic solvent isooctane is used to solubilize the protein RNase T_1. The physicochemical properties of the entrapped protein have been studied using intrinsic tryptophan fluorescence and far- and near-UV CD. These studies indicate a similar structure for the protein in reverse micelles and in pH 7.0 buffer. Thermal unfolding has been studied as a function of W_o, the molar ratio of water to AOT, in the solution. Measuring the change in fluorescence intensity as a function of temperature, we observe a reversible transition for W_o in the range 5−12. Heating rate dependencies carried out on these transitions (0.6−3.0 °C/min) indicate that the transition temperature and the apparent van't Hoff enthalpy change depend on the scanning rate as well as on W_o. The values of the transition temperature, T_m, and the enthalpy change, $\Delta H°_{un}$, extrapolated to an infinitely slow scanning rate, are analyzed considering the electrostatic interaction of the charged residues of the protein with the charges of the surfactant molecules forming reverse micelles, the variation of the size of the reverse micelles, and the relative rates of unfolding, refolding, and irreversible denaturation.

Reverse micelles are spheroidal aggregates formed by certain amphiphilic molecules in apolar solvents. Reverse micelles possess a polar core (formed by the head groups of the amphiphiles) and hence can entrap aqueous pools (Luisi *et al*. 1988; Luisi & Magid 1986; Verhaeret *et al*., 1992). In recent years there have been a number of attempts to solubilize proteins in reverse micelles (Pileni, 1981; Steinman *et al*., 1986; Barbaric & Luisi, 1981; Wolf & Luisi, 1979; Hilhorst *et al*., 1982; Meir & Luisi, 1981; Martinek *et al*., 1981, 1982; Visser *et al*., 1994; Krei & Hustedt, 1992; Hagen *et al*., 1990a,b; Ferreire & Gratton, 1990; Forney & Glatz, 1995; Choudhari & Spirovska, 1994; Guz & Wasylewski, 1994). The facts that enzymes entrapped within reverse micelles are stable, optically transparent, and, importantly, that the encapsulated proteins retain activity, make such systems important for practical reasons and make them good model systems for understanding the properties of proteins in a cell-like environment.

Reverse micelles have been formed with a variety of surfactants and apolar phases, including AOT,[1] CTAB, and EO_4C_{12} as surfactants and isooctane (IO), *n*-octane, heptane, phospholipids, and hexadecane as apolar phases. AOT/IO/H_2O is a widely employed reverse micellar system due to its stability under a large variety of conditions and its capability of solubilizing relatively large amounts of water (Luisi & Magid, 1986). The term W_o refers to the ratio of the number of moles of entrapped water/moles of surfactant in a reverse micelle.

In order to understand the conformational behavior of proteins inside reverse micelles, one must employ methods that can directly probe the entrapped protein. Spectroscopic techniques are the methods of choice (Vos *et al*., 1987). NMR spectroscopy, which is the most powerful solution structural tool, suffers from the requirement of large concentrations of the protein to obtain good quality spectra (Shapiro *et al*., 1989). Circular dichroism (CD) spectroscopy has been used to obtain information about the secondary structure (far-UV region) and tertiary structure of proteins (near-UV region). A common observation is that the ellipticity of proteins and peptides in the far-UV range increases in magnitude with entrapment, indicating an increase in α-helix content (Barbaric & Luisi, 1981; Nicot *et al*., 1985; Steinmann *et al*., 1986; Gallay *et al*., 1987; Lenz *et al.*, 1995); for some proteins, however, essentially no change in secondary structure appears to occur upon entrapment (Wolf & Luisi, 1979). For the near-UV region, a change in spectral feature has been observed for some proteins in reverse micelles, but not for other proteins (Barbaric & Luisi, 1981; Steinmann *et al*., 1986; Lenz *et al*., 1995), indicating that the tertiary structure is altered in some cases.

Steady-state and time-resolved fluorescence methods have also been widely used to characterize the dynamics and microenvironment of entrapped probe molecules, including proteins (Wong *et al.*, 1976; Nicot *et al*., 1985; Galley *et al*, 1987; Dorovska-Taran *et al.*, 1993; Visser *et al*., 1994; Davis *et al.*, 1994). Like in the case of CD, fluorescence studies give variable results for different proteins and peptides, due to the effect of the micellar environment on the structure of the protein and interactions with the inner micellar interface and solvent. Entrapment of proteins usually appears to decrease the overall rotational correlation time of the protein and its tryptophan side chain (Gallay *et al*., 1987; Marzola & Gratton, 1991; Bhattacharyya & Basak, 1993; Dorovska-Taran *et al.*, 1993); for some proteins there is also an increase in extent of segmental rotational motion of the tryptophan side chain, as compared to that for the protein in buffer (Visser *et al.*, 1994). Fluorescence intensity and anisotropy decay parameters for proteins, as well as the maxima for their emission spectra, are usually found to depend on the W_o for the reverse micelle.

[†] This research was supported by National Science Foundation Grant MCB 94-07167.

* To whom correspondence should be addressed.

[⊗] Abstract published in *Advance ACS Abstracts,* March 1, 1996.

[1] Abbreviations: AOT, bis(2-ethylhexyl)sodium sulfosuccinate; CTAB, cetyltrimethylammonium bromide; EO_4C_{12}, tetraethyleneglycol dodecylether; NMR, nuclear magnetic resonance; RNase T_1, ribonuclease T_1; UV, ultraviolet; W_o, moles of entrapped water per mole of surfactant.

0006-2960/96/0435-4094$12.00/0

Studies of the thermodynamics of entrapped proteins have dealt primarily with the process of uptake (or solubilization) of proteins into reverse micelles (Wolbert *et al.*, 1989; Dekker *et al.*, 1991; Andrews *et al.*, 1994). Collectively, these studies have shown that the charges on both the protein and surfactant, as well as ionic strength and the size of the reverse micelle, have an effect on the rate and amount of protein that can be entrapped. The thermal unfolding of proteins (ribonuclease A, cytochrome *c*, and lysozyme) in AOT/IO/H_2O reverse micellar system has been studied by Battistel *et al*. (1988) using differential scanning calorimetry (DSC). These researchers observed single thermal transitions for these proteins; the transitions were not reversible. It was observed for the three proteins that there was an optimum W_o, above which destabilization occurred and enzymatic activity decreased.

Despite a large number of studies on proteins entrapped in reverse micelles, a number of important biophysical issues are still not completely understood. Can a protein reversibly fold within reverse micelles? What is the effect of entrapment on the stability and other thermodynamic properties of proteins? What is the effect of charge and protein size on its uptake into reverse micelles? What is the role of the entrapped water on the structure, stability, and dynamics of the native and unfolded states of entrapped proteins? What is the effect of entrapment on the kinetics of unfolding of a protein?

In this paper we present a spectroscopic characterization, using CD (both near- and far-UV) and fluorescence spectroscopy, of the protein RNase T_1 entrapped in AOT/IO reverse micelles at neutral pH. The reasons for choosing RNase T_1 for this study will be made clear in the Discussion. Also, we present thermal unfolding studies of the entrapped protein at different heating rates and for a range of W_o values. Analysis is based on a two-state reversible process, which is viewed as an extreme case of a kinetic model containing native, unfolded, and denatured species. We will show that two-state behavior is observed under certain conditions, enabling us to characterize the thermodynamics of protein folding in a reverse micelle. Since the negatively charged interface and the structured water pools inside reverse micelles share features with the cellular milieu, reverse micelle systems can be viewed as a model environment for studying the folding of proteins and for exploring certain interactions and forces that do not exist in dilute aqueous solutions.

MATERIALS AND METHODS

Chemicals and Solution Preparation. All the chemicals used in this study are of high-purity grade from Sigma Chemicals (St. Louis, MO). AOT purchased from Sigma was used without further purification. The buffer used in all experiments was 50 mM sodium cacodylate, pH 7.0. The protein RNase T_1 was a gift from Dr. C. N. Pace (Texas A&M University). Stock protein solutions (1−2 mg/mL) were prepared by dissolving lyophilized protein in filtered and degassed buffer; the solutions were then centrifuged before use. The concentration of the protein was determined spectroscopically using an absorption of 1.67 at 278 nm for a 1 mg/mL solution (Hu *et al*., 1992).

Protein micellar solutions were prepared by adding aliquots of the stock protein solution into a 150 mM AOT/IO solution (prepared by dissolving solid detergent directly into the organic solvent). The experimental W_o was achieved by adding additional amounts of the same 50 mM cacodylate buffer in which the protein was prepared. Micellar solutions were prepared by mild hand shaking until a clear solution was obtained. The final protein concentration was ∼1.2 μM (expressed per total volume, organic plus aqueous, in the solution) in all fluorescence experiments.

Spectroscopic Characterization. Intrinsic fluorescence measurements of RNase T_1 were made with a Perkin-Elmer MPF 44A spectrofluorimeter using a 1 cm pathlength cuvette with excitation at 295 nm and with the slit widths of both excitation and emission monochromators set at 5 nm. CD spectra were obtained on an AVIV 62DS spectropolarimeter using a protein concentration of 2 mg/mL. A 1 cm cuvette and a 10 cm cuvette were used, respectively, in the far- and near-UV regions. All the spectra have been recorded at 25 °C with an averaging time of 16 s and with an excitation bandwidth of 0.6 nm. The ellipticity has been expressed as deg cm^2 dmol^{-1}, normalized to the mean residual molecular weight of the protein (Sander & Ts'O, 1971).

Thermal Denaturation Studies. The thermal unfolding studies have been performed by monitoring changes in the steady state fluorescence of the single tryptophan residue, *Trp*-59, of the protein as a function of temperature. These experiments have been performed on a modified AVIV 62DS CD spectropolarimeter, which is capable of monitoring the fluorescence intensity with an additional Hamamatsu 948 photomultiplier tube mounted at right angles to the sample compartment (Ramsay & Eftink, 1994). Tryptophanyl fluorescence was excited at 295 nm and measured at 320 nm using an interference filter. An excitation bandwidth of 0.6 nm was used in all of the experiments. The temperature was controlled with a thermoelectric cell holder, and the temperature in the cuvette was measured with a thermistor probe. The temperature of the thermoelectric cell holder was increased at different heating rates (linear), and the signals from the thermistor probe and the fluorimeter output were digitized and recorded.

Data Analysis. For a simple case of reversible two-state, N ⇌ U, unfolding reaction, where N and U are the native and the unfolded states of the protein, respectively, the thermodynamic relationships for the transition temperature, T_m, the enthalpy change ($\Delta H°_{un}$), entropy change ($\Delta S°_{un}$) and free energy change ($\Delta G°_{un}$) on temperature are well-known (Privalov, 1979, 1992; Pace, 1986; Pace *et al*., 1992; Eftink, 1994, 1995). Below we reproduce these basic equations for completion.

To obtain estimates of T_m and $\Delta H°_{un}$, raw data were fitted *via* nonlinear least-square (NLLSQ) analysis, with six fitting parameters, Y_N, m_N, Y_U, m_U, $\Delta H°_{un}$, and T_m (= $\Delta H°_{un}/\Delta S°_{un}$), with the equations (Eftink, 1994, 1995)

$$Y = (Y_N + m_N T)X_N + (Y_U + m_U T)(1 - X_N) \qquad (1)$$

$$X_N = 1/(1 + e^{-\Delta G°_{un}/RT}); \quad \Delta G°_{un} = \Delta H°_{un} - T\Delta S°_{un} \qquad (2)$$

where Y is the experimentally observed optical signal at a given temperature, Y_N and Y_U represent the signals of the pure N and U states at 0 °C, and m_N and m_U are the temperature dependencies (assumed to be linear) of these signals (i.e., the slopes) for the N and U states, respectively. R and T have their usual meanings. The solid lines through

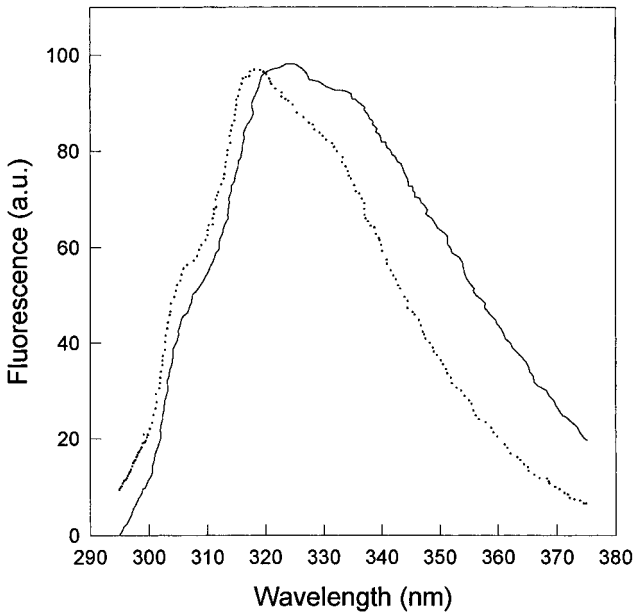

FIGURE 1: Fluorescence spectrum of RNase T_1 in the buffer (50 mM cacodylate, pH 7, 25 °C) (- - -) and in the reverse micelles (150 mM AOT/IO/W_o = 3.7, 25 °C) (• • •).

the data points in Figures 3 and 4 represent the results such fits. The free energy change for the unfolding transition at 20 °C was obtained using the relationship in which where ΔC_p is the change in the heat capacity for the transition,

$$\Delta G^\circ_{un} = \Delta H^\circ_{un}(1 - T/T_m) + \Delta C_p[T - T_m - T\ln(T/T_m)] \quad (3)$$

which was obtained as the slope of the plot of ΔH°_{un} vs T_m obtained at different W_o values (see Results).

RESULTS

Steady-State Fluorescence Studies. Figure 1 shows the fluorescence spectrum of RNase T_1 in buffer (50 mM cacodylate, pH 7, 25 °C). The emission spectrum has the characteristic blue fluorescence of this protein with a maximum at around 325 nm (Longworth, 1968; Yamamoto & Tanaka, 1970). Included in the same figure is the fluorescence spectrum of the protein in reverse micelles (150 mM AOT/IO, 25 °C, W_o = 4.94). The fluorescence of RNase T_1 in reverse micelles shows a blue-shift (about 3 nm) in the emission maximum at low W_o compared with the spectra in the buffer. This shift decreases by increasing the water content; at high water contents (W_o > 11.1) the maximum of the emission spectrum approaches the value of protein in the buffer. The characteristic shoulders in the emission spectra of RNase T_1 are observed at all W_o values over the range 5−12.

Circular Dichroism Studies. Far- and near-UV CD spectra are shown in Figure 2a,b, respectively. Included in the same figure are the spectra of the protein in buffer (solid line) and in reverse micelles (open symbol) with different W_o. The far-UV CD spectra in reverse micelles are quite similar to that in the buffer. This behavior is somewhat different from what has been observed for some other proteins, where an increase in the α-helical content has been noticed upon entrapment in AOT reverse micelles (Nicot *et al.*, 1985; Gallay *et al.*, 1987; Luisi & Magid, 1988). The striking similarity in the aromatic region of the spectrum suggests that the protein retains its tertiary structure, in the region of W_o investigated in this study. The CD spectra of RNase T_1 in buffer compare well with those reported in the literature (Yamamoto & Tanaka, 1970).

Thermal Transitions of RNase T_1 in AOT Reverse Micelles. Shown in Figure 3a is the thermal unfolding transition of RNase T_1 obtained by monitoring the decrease in the fluorescence intensity of the protein in 50 mM cacodylate, pH 7, at a heating rate of 1.2 °C/min. The thermal transition temperature, T_m = 326 ± 0.5 K, obtained in the present study (from nonlinear least-squares fits of eq 1) agrees well with the value reported in the literature (Plaza del Pino *et al.*, 1992). When the protein unfolds, its fluorescence intensity decreases significantly and shifts to the red ($\lambda_{max} \approx$ 345 nm for the thermally unfolded state). The protein is found to regain its initial intensity when cooled quickly from 65 °C, a temperature well above the transition (data not shown). A heating rate dependence of the apparent T_m (see below) suggests that the reversibility is much better when higher heating rates are employed and the sample is not left for long durations in the thermally unfolded state (Pace *et al.*, 1992).

Shown as Figure 3b are data that support the reversibility of the thermal unfolding of RNase T_1 in reverse micelles, with W_o = 4.94 as a typical example. The protein, which was unfolded by increasing the temperature at a constant rate of 1.2 °C/min (△), was cooled to 20 °C at a rate of 80 °C/min and was re-unfolded by heating at a rate of 1.2 °C/min (▽). This shows that the unfolding transition is repeatable, since the recovered T_m values are within experimental error of one another. Such repeatablity is usually taken as an indication of reversibility. (Actually, as will be shown below, the transitions are not exactly at equilibrium during the scans.) The fluorescence intensity decreases and the fluorescence emission maximum shifts to the red, as is observed for the protein in buffer. Figure 4 shows a family of thermal scans at different W_o values. For clarity only a few data sets have been shown. A constant heating rate of 0.6 °C/min has been used in obtaining these transitions.

A study of the dependence of the transition on thermal heating rate, varied from 0.6 to 3.0 °C/min with an interval of 0.6 °C, has been carried out at different W_o values in order to ascertain whether equilibrium is being reached during the thermal scans. At the higher heating rates the transitions were easily repeatable. Figure 5 (panels a and c) shows a plot of the apparent transition temperature and the apparent van't Hoff enthalpy change of the transition versus scanning rate at different W_o values. Both the apparent T_m and the apparent ΔH°_{un} were found to be dependent on the scanning rate. We have extrapolated such apparent ΔH°_{un} and T_m data to zero scan rate to obtain values that should more nearly correspond to equilibrium values. These extrapolated T_m and ΔH°_{un} values are plotted in Figure 5 (panels b and d) as a function of W_o and are tabulated in Table 1.

The extrapolated ΔH°_{un}, for various W_o, were plotted versus the extrapolated T_m (not shown). The slope of this linear plot, which provides an estimate of the change in the heat capacity, ΔC_p, has a value of 1.2 ± 0.2 kcal/mol·deg. This value is very close to the value calculated based on the "thumb rule" [that each of the amino acids contribute 12 cal/mol/deg to the total heat capacity change (Pace *et al.*, 1992)] and with the calorimetrically determined value of 1.16 kcal/mol·deg for the thermal unfolding of RNase T_1 in

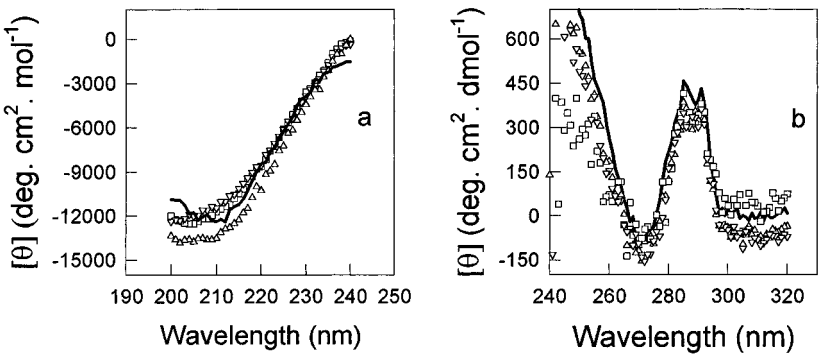

FIGURE 2: (a) Far-UV CD spectra of RNase T_1 in the buffer (solid curve) and in reverse micelles. W_o = 4.94 (▽); 8.94 (□); 12 (△). (b) Near-UV CD spectra of RNase T_1 in the buffer (solid curve) and in reverse micelles. W_o = 4.94 (▽); 8.94 (□); 12 (△).

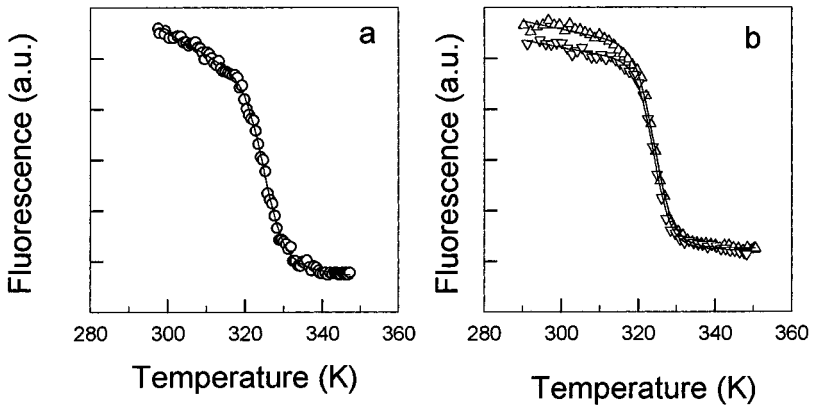

FIGURE 3: (a) Thermal unfolding of RNase T_1 in 0.05 M cacodylate, pH 7, heating rate 1.2 °C/min. (b) Reversible thermal unfolding of RNase T_1 in reverse micelles with W_o = 6.17. 1.2 μM RNase T_1, dissolved in pH 7.0 50 mM cacodylate, was unfolded by increasing the temperature at a rate of 1.2 °C/min (△). After complete denaturation (65 °C), the solution was cooled to 25 °C at rate of 80 °C/min and it was re-unfolded at the same rate of 1.2 °C/min (▽). Solid line through the data is a theoretical fit to eq 2.

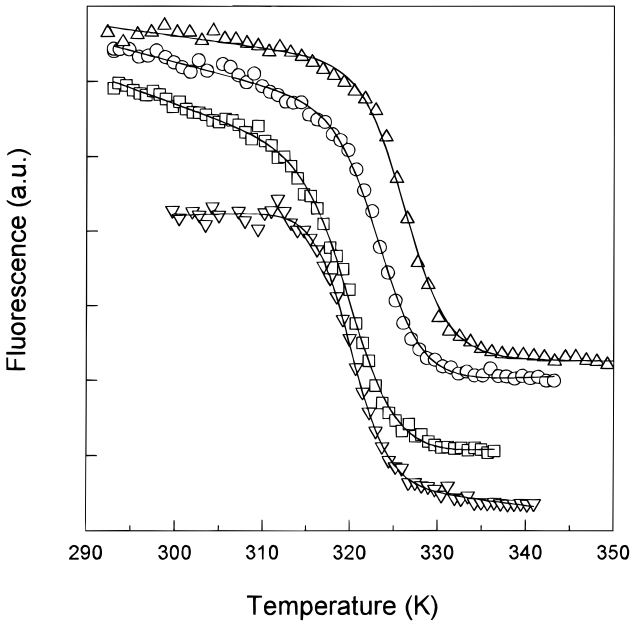

FIGURE 4: Thermal unfolding curves of RNase T_1 in reverse micelles at different W_o values. Solid line through the data is a theoretical fit to eq 2. W_o = 0 (○); 4.94 (△); 8.94 (□); 12 (▽).

solution at pH 5.3 (Plaza del Pino *et al.*, 1992). The values of the change in free energy, $\Delta G°_{un}$, for the unfolding of the protein at 298 K, evaluated using this value of ΔC_p (and eq 3) are also included in the Table 1. In contrast to $\Delta G°_{un}$ values found for entrapped RNase A, lysozyme, and cytochrome c, which are greatly destabilized within AOT reverse micelles (Battistel *et al.*, 1988), we find that RNase T_1 has nearly the same $\Delta G°_{un}$ for unfolding in the micellar and dilute aqueous environments, with there being a slight trend for $\Delta G°_{un}$ to decrease with increasing W_o.

Attempts were made to characterize the thermal transition of entrapped RNase T_1 at W_o values less than 4.5. Although the solutions were quite clear and good fluorescence spectra were obtained, it was difficult to obtain reproducible thermal transitions which were strictly two-state and results for the low W_o values are not shown. Also at certain high W_o values (for example, at 13.6), thermal scans at high heating rates (e.g., 3 °C/min) revealed transitions that were not two-state and that indicated the accumulation of at least one intermediate species. These results will not be presented at this time.

DISCUSSION

Reversible thermal unfolding of RNase T_1 in buffer has been widely studied (Plaza del Pino *et al.*, 1992; Pace, 1988, 1992; Pace *et al.*, 1992). To our knowledge, this is the first report of the study of RNase T_1 in reverse micelles. Spectroscopic evidences presented in this study strongly suggest that the protein retains its native structure in AOT/IO reverse micelles. Thermal unfolding studies indicate that the transitions are essentially two-state processes and are reversible under certain conditions (W_o between 5 and 12 and scan rates between 1 and 3 °C/min). Moreover, the apparent T_m and $\Delta H°_{un}$ are found to depend on both the value of W_o and the scanning rate.

The stability of a protein in a buffer solution is affected by a number of interactions, including intramolecular hy-

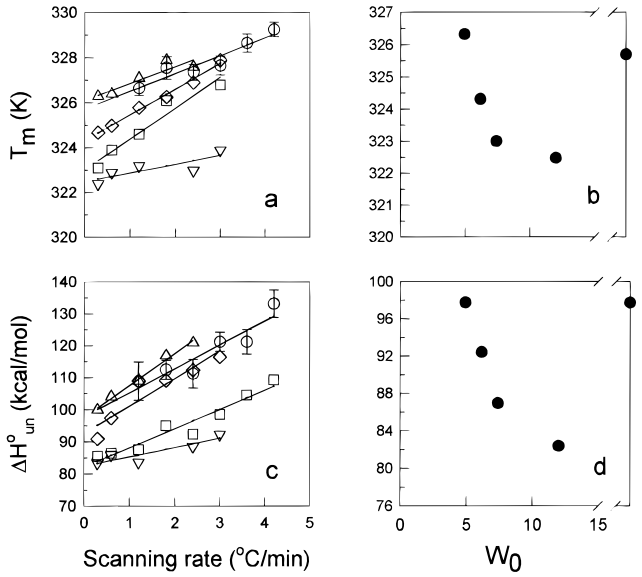

FIGURE 5: Experimental transition temperatures (a) and van't Hoff ΔH°_{un} (c), as a function of scanning rate in different micellar systems. $W_o = 0$ (○); 4.94 (△); 6.17 (◇); 8.94 (□); 12 (▽). Solid lines through the data points are best fits to a linear equation. Error bars for the apparent T_m and ΔH°_{un} values are shown for one data set. Panels b and d show the variation of extrapolated T_m and ΔH°_{un} versus W_o. The values of T_m and ΔH°_{un} are the extrapolated values to zero scanning rate. The data point after the break corresponds to that of protein in the buffer.

Table 1: Equilibrium Values of the Thermodynamic Parameters[a] Evaluated for Thermal Transition of RNase T_1 in Buffer (50 mM Cacodylate, pH 7) and in Reverse Micelles of 150 mM AOT/IO at Different W_o Values

W_o	T_m (K)[a]	ΔH°_{un} (kcal/mol)	ΔG°_{un} at 298 K (kcal/mol)
buffer only	325.7	97.7	6.9
4.94	326.3	97.4	7.0
6.17	324.3	92.4	6.2
7.40	323.0	86.9	6.2
12.0	322.5	82.4	5.2

[a] The average confidence interval for T_m values is ±0.5 °C, that for ΔH°_{un} values is ±5 kcal/mol, and that for ΔG°_{un} is ±0.1 kcal/mol.

drogen bonds, electrostatic interactions, hydrophobic interactions, etc., which counterbalance the decrease in configurational entropy associated with the native state. The stability of a protein in reverse micelles involves not only the above interactions but also the interaction of the charged residues of the proteins with the charges on the surfactant, the possible interactions with the apolar phase, and the confining effect of the micellar walls. Thus, the structural and thermodynamic stability of the protein in reverse micelles is seen as a delicate balance of a number of interactions, some of which are different than those in dilute aqueous solution and which may more closely mimic the environment that a protein experiences within a cell. In this section we will expand upon the above points by (1) discussing our data regarding the structure of entrapped RNase T_1, (2) discussing the various interactive forces that are believed to pertain to entrapped proteins, and (3) discussing our thermodynamic data for the RNase T_1/AOT system and the implications of the observed thermal scan rate dependence.

Similarity in the Structure of the Protein in the Buffer and in Reverse Micelles. The entrapped protein RNase T_1 in reverse micelles appears to retain the same structure as that of the protein in buffer as evidenced by the similarity in their spectroscopic properties (Figures 1 and 2). Similar CD spectra in the aromatic and peptide regions indicate that the microenvironment around the aromatic residues and the secondary structure of the protein are not significantly altered when the protein is within the reverse micelles. A slight blue-shift is observed in the fluorescence of *Trp*-59 of the protein in the reverse micelles (Figure 1). This finding is consistent with the data reported to date for many proteins (Nicot *et al.*, 1985; Marzola & Gratton, 1991; Bhattacharyya & Basak, 1993). The blue-shift observed in the emission maximum of other proteins and peptides has been taken as an indication that the entrapped water molecules are somewhat restricted and have a reduced ability for orientational relaxation around the excited-state dipoles of the fluorophores (Bhattacharyya & Basak, 1993). Since *Trp*-59 in RNase T_1 is present in the interior of the protein, the small blue-shift in its emission maximum might indicate a bulk dielectric effect rather than a consequence of the altered hydration states of the fluorophore in reverse micelles. Importantly, the fine structured fluorescence, together with the structured aromatic CD spectrum, suggest that the environment around *Trp*-59 remains highly and asymmetrically organized when the protein is entrapped.

In unpublished time-resolved fluorescence studies, we have found that the mean fluorescence lifetime of *Trp*-59 in entrapped RNase T_1 is relatively unchanged from its value in buffer. Also, anisotropy decay data show that the rotational motion of entrapped protein is described relatively well, in W_o range of 10−25, by a single rotational correlation time, which decreases with increasing W_o. These results support the above interpretation that the protein retains its native structure inside the AOT reverse micelles.

Features of the Micellar Environment and Their Potential Effect on Protein Stability. As mentioned in the opening of the Discussion, proteins that are in a reverse micellar environment experience forces that are different than those in an aqueous solution. The pool-water molecules are expected to be more structured than bulk-water, the inner walls of the micelle are charged, there may be interactions between amino acid side chains and the apolar hydrocarbons at the interface, and the size of the micelles may play a role in confining the conformational space available to both of the native and unfolded states of the protein. Here we will discuss these interactive forces as they may relate to the thermodynamics of the unfolding of an entrapped protein.

Solvent Properties of Pool-Water. One of the first models proposed to understand the behavior of proteins in reverse micelles and to explain the process of uptaking guest molecules was the water-shell model (Wolf & Luisi, 1979). According to this model, protein is surrounded by one or more layer of water molecules that protect the macromolecule from the denaturing effects of the surfactant molecules and organic solvents. The aqueous pool of reverse micelles is assumed to contain different water populations, which are in rapid exchange with one another and which are characterized by different motional properties and degrees of organization (Luisi *et al.*, 1984). This model envisages at least three different types of water molecules with varying properties of dielectric constant, viscosity, polarizability, etc. These types are (1) the water of the aqueous solution (bulk phase water, which occurs in partitioning experiments), which is least structured; (2) the interfacial-water, which

interacts with the polar charged groups (electrostriction) of the surfactant molecules lining the inner surface of the reverse micelle; and (3) pool-water (inside the core of the reverse micelle), which is proposed by Luisi and co-workers to be most structured. The rationalization given for the spontaneous uptake of proteins from the bulk phase into the micellar environment is that this process introduces disorder in the structure of pool-water molecules, thus causing an increase in entropy of the system. The water-shell model also predicts the size of reverse micelles, which is supported by both theoretical and experimental data (Luisi & Magid, 1988). Regardless of the validity of this model, the properties of the internal water molecules are likely to be of importance in determining the strength of the hydrophobic effect and of hydrogen bonds, as they pertain to the native and unfolded states of proteins.

Effect of Size of the Reverse Micelle. In the case of reverse micelles of AOT we assume that the average sizes of the reverse micelles change from 15 to 25 Å (internal radius of pool) when W_o changes from 4 to 15 (Luisi & Magid, 1988). At $W_o \geq 5.0$, the radius of the water pool of the reverse micelles is approximately equal to or larger than the radius of RNase T_1 (which is about 17 Å). When W_o is around 5−6, there probably are just enough water molecules available to hydrate both the surfactant and protein molecules; hence competition exists between the two for hydration.

If it is assumed that a reverse micelle has a fixed volume, then there may also be an effect of volume confinement on the structural states of the protein. As suggested by Minton (1992, 1995), macromolecules that exist within a confined volume tend toward their state of minimum hydrodynamic volume. That is, an unfolded protein will have less conformational space available to explore inside a reverse micelle; consequently, it is expected that the more compact native state will be stabilized by this confinement effect. This is purely a statistical effect and does not include specific effects of interactions with solvent and the charged walls (see below). It is uncertain, however, whether a reverse micelle can be considered to have a fixed volume, or, if in a population of micelles, whether some can grow in volume at the expense of other micelles to accommodate an entrapped macromolecule.

Effect of Electrostatic Interactions with the Inner Micellar Wall. If the protein is unfolded, then the amino acid residues are exposed not only to water but also to the negatively charged environment of the reverse micelles (in the case of AOT micelles). If the protein is positively charged (or, in general, oppositely charged), then there will be electrostatic interactions between the inner surface of the micelles and the protein, in both its native and unfolded states. Such interactions are partially the basis for the favorable solubilization of some proteins into reverse micelles. However, these interactions may also be responsible for the destabilization of the native state and irreversible thermal unfolding that has been seen for certain proteins. For example, in the DSC study by Battistel *et al*. (1988), the three proteins, ribonuclease A (pI = 7.8), cytochrome c (pI = 10.6), and lysozyme (pI = 11), were all positively charged at the experimental pH of 3.3. In each case the protein appeared to be destabilized by incorporation into AOT reversed micelles (as indicated by a decrease in their apparent T_m) and the thermal transitions were irreversible. Interactions between positively charged amino acid side chains and the negatively charged sulfosuccinate groups of the surfactant would be expected to hold the unfolded protein to the inner walls of the micelle (possibly enabling apolar amino acid side chains to then insert into the hydrocarbon phase, perhaps involving the induction of amphipathic helical regions in the unfolded state). If the protein is negatively charged (or has a like charge, compared to that of the surfactant), then one would expect to see a lower degree of solubilization into AOT reverse micelles, and one would expect the interactions between the inner wall and the protein to be repulsive for both the native and unfolded states. As mentioned above with regard to the volume confinement effect, an unfolded protein is expected to have a larger hydrodynamic radius and thus interactions with the unfolded state might be more significant, than those with the native state. Consequently, one would expect that the inner surface charge to stabilize the more compact native state due to both the confinement effect and to electrostatic repulsion. As the size of the reverse micelle increases, the electrostatic interactions, whether favorable or repulsive, are expected to diminish for both conformational states. In the present study, with a negatively charged protein (pI = 2.9, at the experimental pH of 7) in an AOT reverse micelle, T_m and $\Delta G°_{un}$ are expected to decrease as W_o increases. This is the observed trend, as shown in Table 1. The observed non-reproducibility and the possible multiphasic character of thermal transitions, when W_o values less than 4 are employed, may be directly related to the smaller and heterogeneous size of reverse micelles at low W_o values. If the size of the reverse micelles is small compared to the size of the protein, then nonspecific interactions would be expected. We also note that at these smaller W_o values there are more empty reverse micelles, and the unknown effect of temperature on them may add to complications.

Reasons for Selecting RNase T_1. In trying to find a reverse micellar system that would show reversible thermal unfolding and for which the structure of the entrapped state could be determined with some certainty using optical spectroscopic methods, several attributes are favorable for RNase T_1. The characteristic tryptophan fluorescence spectra, having a blue emission and fine structure, in the native state, as well as the characteristic aromatic CD spectrum, enable us to show that entrapped protein most probably retains its native structure. Likewise, the large drop in fluorescence and red-shift in the emission maximum enable us to identify and track the thermal unfolding transition. As mentioned above, the fact that this protein has a net negative charge at neutral pH seems to be key for maintaining the stability of the more compact native state within the negatively charged AOT reverse micelle. Finally, the fact that the unfolding of RNase T_1 occurs slowly prompted us to study the scan rate dependence of the thermal unfolding process, the results of which are discussed below.

Kinetically Controlled Thermodynamic Model. An emphasis of this study is the reversible unfolding of RNase T_1 and the investigation of whether or not the transition is kinetically controlled. Thermal transitions of proteins may be irreversible if they are scanned sufficiently slowly and are held at post-transition temperatures for a long period of time. Such irreversibility results if the unfolded state undergoes some reaction to form a denatured state (here defined as a state that can not refold to a native-like state on

the experimental time scale). The scan rate dependence on a thermal denaturation is an indication of whether a transition is limited by, or coupled to, a kinetic process, which may be either the unfolding transition itself or an irreversible reaction converting the unfolded state to a denatured state (Lepock *et al.*, 1992). RNase T_1 is known to exhibit slow kinetics when denatured by various denaturants (Plaza del Pino *et al*., 1992; Keifaber *et al*., 1990). When RNase T_1 is entrapped in AOT reverse micelles, its apparent T_m and $\Delta H°_{un}$ for are scan rate dependent and the thermal transitions are reversible for micelles in the range $W_o = 5-12$. When W_o is increased further, the transitions become only partially reversible and are not strictly two-state. We consider the transitions to be treated by the following kinetic model.

$$N \underset{k_2}{\overset{k_1}{\rightleftharpoons}} U \xrightarrow{k_3} D$$

where N, U, and D are the native, unfolded, and denatured forms of the protein and k_1, k_2, and k_3 are the microscopic rate constants characterizing the formation of U, N, and D, respectively. Thus, the thermal transition can be looked upon as a kinetic process in which the relative magnitudes of the rate constants control the formation of the various species. In the case of proteins in aqueous solution, possible reasons for the formation of a denatured species vary from the formation of aggregates, improper disulfide bond formation, irreversible loss of cofactors, oxidation of side chains, or other covalent modifications.

For RNase T_1 in AOT reverse micelles, at low W_o values we can assume that k_1 and $k_2 > k_3$, because irreversible denaturation does not appear to occur. If k_3 is small, then no appreciable amount of the D state will form during the experiment. As mentioned above, electrostatic repulsion between the negatively charged unfolded protein and the negatively charged surfactant interface may favor refolding. In other words, k_2 may have a high value at low W_o, shifting the equilibrium to left. Thus reversibility may be a consequence of the relative magnitudes of the rate constants k_1, k_2, and k_3 for the entrapped proteins at different W_o values. When k_3 is small, the transition will be a simple two-state reversible process. As W_o increases, more and more water molecules are added into the reverse micelles, the size of the reverse micelles also increases, and the unfolded protein may be shielded from the unfavorable interaction with the surfactant. Thus, the unfolded state may be more stable at higher W_o. According to this view, the value of $\Delta G°_{un}$ should decrease at higher W_o, which is experimentally observed to be the case. However, this condition also increases the opportunity for irreversible denaturation, leading to a loss of reversibility. Although we have not done a detailed study of the influence of temperature on the kinetics of formation of D, it appears that k_3 depends on temperature, increasing at higher temperatures.

CONCLUSIONS

Spectroscopic characterization of the protein RNase T_1 in reverse micelles strongly suggests that the protein retains the same conformation as that in the buffer. Thermal unfolding studies of the protein RNase T_1 has been carried out by monitoring the accompanying fluorescence change. This protein exhibits reversible unfolding transitions at all W_o values investigated in the study. The free energy of stability, $\Delta G°_{un}$, and the enthalpy change for unfolding, $\Delta H°_{un}$, for RNase T_1 are found to be approximately the same for the entrapped protein as the corresponding thermodynamic parameters for the thermal unfolding of the protein in dilute aqueous solution. However, $\Delta G°_{un}$ and $\Delta H°_{un}$ are found to depend on the size of the reverse micelle, which must be related to the number of water molecules within the reverse micelles and the interaction between the charged residues of the unfolded protein and the negatively charged surfactant. The transition temperature is higher and the transition is more cooperative in the range of $W_o \approx 5$, compared to other W_o values investigated in this study. In the cases where the $W_o < 5$, we expect nonspecific interactions, since the reverse micelles are smaller in diameter and they cannot easily accommodate the protein molecules. These are manifested as non-reproducible thermal transitions at low W_o values. At higher W_o values, it appears that the unfolded state is stabilized but that other irreversible reactions lead to an irreversible U → D step. The whole process can be accounted for using a kinetically controlled thermodynamic model in which the rates of unfolding, refolding, and irreversible denaturation vary as W_o and the heating rates are varied.

ACKNOWLEDGMENT

We thank Dr. C. N. Pace, Texas A&M University, for providing us with the protein.

REFERENCES

Andrews, B. A., Pyle, D. L., & Asenjo, J. A. (1994) *Biotechnol. Bioeng. 43*, 1052−1058.
Barbaric, C. S., & Luisi, P. L. (1981) *J. Am. Chem. Soc. 103*, 4239−4244.
Battistel, E., Luisi, P. L., & Rialdi, G. (1988) *J. Phys. Chem. 92*, 6680−6685.
Bhattacharyya, K., & Basak, S. (1993) *Biophys. Chem. 47*, 21−31.
Choudhari, J. B., & Spirovska (1994) *Biotechnol. Tech. 8*, 909.
Davis, D. M., McLoskey, D., Birch, D. J. S., Swart, R. M., Gellert, P. R., & Kittlety, R. S. (1994) *Proc. SPIE—Int. Soc. Opt. Eng. 2137*, 331−342.
Dekker, M., van't Riet, K., Van Der Pol, J. J., Baltussen, J. W. A., Hilhorst, R., & Bijsterbosch, B. H. (1991) *Chem. Eng. J. 46*, B69−B74.
Dorovska-Taran, V. N., Veeger, C., & Visser, A. J. V. G. (1993) *Eur. J. Biochem. 211*, 47−55.
Eftink, M. R. (1994) *Biophys. J. 66*, 482−501.
Eftink, M. R. (1995) *Methods Enzymol. 259*, 487−512.
Forney, C. E., & Glatz, C. E. *(1995) Biotechnol. Prog. 11*, 260−264.
Gallay, J., Vincent, M., Nicot, C., & Waks, M. (1987) *Biochemistry 26*, 5738−5747.
Guz, A., & Wasylenski, Z. (1994) *J. Protein Chem. 13*, 394−399.
Hagen, A. J., Hatton, T. A., & Wang, D. I. C. (1990a) *Biotechnol. Bioeng. 35*, 955−965.
Hagen, A. J., Hatton, T. A., & Wang, D. I. C. (1990b) *Biotechnol. Bioeng. 35*, 966−975.
Hilhorst, R., Laane, C., & Veeger, C. (1982) *Proc. Natl. Acad. Sci. U.S.A. 79*, 3927−3930.
Hu, C. Q., Sturtevant, J. M., Thomson, J. A., Erickson, R. E., Imre, V. E., & Luisi, P. L. (1982) *Biophys. Biochem. Res. Commun. 107*, 538−545.
Kiefhaber, T., Schmid, F. X., Renner, M., Hinz, H. -J, Hahn, U., & Quaas, R. (1990) *Protein Sci. 29*, 8250−8257.
Krei, G. A., & Hustedt, H. (1992) *Chem. Eng. Sci. 47*, 99−111.
Lenz, V. J., Federwisch, M., Gattner, H.-G., Brandenburg, D., Höcker, H., Hassiepen, U., & Wollmer, A. (1995) *Biochemistry 34*, 6130−6141.

Lepock, J. R., Ritchie, K. P., Kolios, M. C., Rodahl, A. M., Heinz, K. A., & Kruuv, J. (1992) *Biochemistry 31*, 12706−12712.
Longworth, J. W. (1968) *Photochem. Photobiol. 7*, 587−592.
Luisi, P. L., & Magid, J. (1986) *CRC Crit. Rev. Biochem. 20*, 409−474.
Luisi, P. L., Luithi, P., Tomka, I., Prenosil, J., & Pande, A. (1984) *Enzyme Eng. 7*, 549−557.
Luisi, P. L., Giomini, M., Pileni, M. P., & Robinson, B. H. (1988) *Biophys. Biochim. Acta 947*, 209−246.
Martinek, K., Levashov, A. V., Khmelnitsky, Y. L., Klyachko, N. L., & Berezin, I. V. (1982) *Science 218*, 889−893.
Martinek, K., Levashov, A. V., Klychko, N., Khmelmitsky, Y. L., & Berezin, I. V. (1986) *Eur. J. Biochem. 155*, 453−468.
Marzola, P., & Gratton, E. (1991) *J. Phys. Chem. 95*, 9488−9495.
Meier, P., & Luisi, P. L. (1980) *J. Solid Phase Biochem. 5*, 269−282.
Minton, A. P. (1992) *Biophys. J. 63*, 1090−1100.
Minton, A. P. (1995) *Biophys. J. 68*, 1311−1322.
Nicot, C., Vacher, M., Vincent, M., Gallay, J., & Waks, M. (1985) *Biochemistry 24*, 7024−7032.
Pace, C. N. (1986) *Methods Enymol. 131*, 198−200.
Pace, C. N. (1992) *Biochemistry 31*, 4876−4882.
Pace, C. N., Shirley, B. A., & Thomson, J. A. (1992) in *Protein Folding* (Creighton, T. E., Ed.) pp 311−330, W. H. Freeman & Co., New York.
Pileni, M. P. (1981) *Chem. Phys. Lett. 81*, 603−605.
Plaza del Pino, I. M., Pace, C. N., & Freire, E. (1992) *Biochemistry 31*, 11196−11202.
Privalov, P. L. (1979) *Adv. Protein Chem. 33*, 167−241.
Privalov, P. L. (1992) in *Protein Folding* (Creighton, T. E., Ed.) pp 83−126, W. H. Freeman & Co., New York.
Ramsay, G. D., & Eftink, M. R. (1994) *Biophys. J. 66*, 516−523.
Sander, C., & Ts'o (1971) *Biochemistry 10*, 1953−1966.
Shapiro, Y. E., Budanov, N. A., Levashov, A. V., Klyachko, N. L., Khmelnitsky, Y. L., & Martinek, K. (1989) *Coll. Czech. Chem. Commun. 54*, 1126−1134.
Steinman, B., Jackle, H., & Luisi, P. L. (1986) *Biopolymers 25*, 1133−1156.
Verhaeret, R. M. D., Hilhorst, R., Visser, A. J. V. G., & Veeger, C. (1992) in *Biomolecules in organic solvents* (Gomez-Puyou, A. Ed) pp 133−162, CRC Press, Boca Raton, FL.
Visser, A. J. V. G., van Engelen, J., Visser, N. V., van Hoek, A., Hilhorst, R., & Freedman, R. B. (1994) *Biophys. Biochim. Acta 1204*, 225−234.
Vos, K., Laane, C., & Visser, A. J. W. G. (1987) *Photochem. Photobiol. 45*, 863−878.
Wolbert, R. B. G., Hilhorst, R., Voskuilen, G., Nachtegall, H., Dekker, M., Van't Riet, K. V., & Bijsterbosch, B. H. (1989) *Eur. J. Biochem. 184*, 627−633.
Wolf, P., & Luisi, P. L. (1979) *Biophys. Biochem. Res. Commun. 89*, 209−217.
Wong, M., Thomas, J. K., & Gratzel, M. (1976) *J. Am. Chem. Soc. 98*, 2391−2397.
Yamamoto, Y., & Tanaka, T. (1970) *Biochim. Biophys. Acta 207*, 522−531.

BI952550T